Catalysis Today 157 (2010) 101–106

Contents lists available at ScienceDirect

Catalysis Today

journal homepage: www.elsevier.com/locate/cattod

# Hydrocarbon oxidation by homogeneous and heterogeneous non-heme iron (III) catalysts with $H_2O_2$

G. Bilis [a], K.C. Christoforidis [b], Y. Deligiannakis [b], M. Louloudi [a,*]

[a] Department of Chemistry, University of Ioannina, Department of Chemisry, 45110 Ioannina, Greece
[b] University of Ioannina, Department of Environmental and Natural Resources Management, Laboratory of Physical Chemistry, Pyllinis 9, 30100 Agrinio, Greece

ARTICLE INFO

*Article history:*
Available online 11 May 2010

*Keywords:*
Non-heme iron
Biomimetic catalysis
Hydrocarbon oxidation
$H_2O_2$
Fe–OOH
Low-spin Fe

ABSTRACT

Homogeneous (**L**$Fe^{III}$) and heterogeneous (**L**$Fe^{III}$·$SiO_2$) [**L** = 3-{2-[2-(3-hydroxy-1,3-diphenyl-allylideneamino)-ethylamino]-ethylimino}-1,3-diphenyl-propen-1-ol] catalysts have been synthesized and evaluated catalytically. In $CH_3CN$, both the homogeneous and heterogeneous catalysts were efficient in alkene oxidations. Cyclohexane oxidation provides total yield of 12.1% and 7.3% with an alcohol/ketone (A/K) ratio of 1.75 and 1.60 by the **L**$Fe^{III}$ and the **L**$Fe^{III}$·$SiO_2$ catalysts respectively. UV–vis kinetic data suggest formation of **L**$Fe^{III}$–OOH species. EPR data show that in the presence of $CH_3CN$, low-spin $Fe^{III}$ ($S = 1/2$) centers are formed, which are responsible for the catalytic activity. The heterogeneous **L**Fe·$SiO_2$ catalyst, tested up to 5 re-uses, shows a total yield loss ~4% *per use*, providing the same distribution of oxidation products.



## 1. Introduction

The development of new iron catalysts for hydrocarbon oxidations is attracting synthetic chemists intending to explore new industrial approaches. Nature has evolved iron-enzymes, like non-heme iron oxygenases, capable to carry out hydrocarbon oxidations with high selectivity, under mild conditions. For example, methane monooxygenase [1–3] selectively oxidizes methane to methanol, Rieske dioxygenases [4,5] are capable of stereospecific dihydroxylation of arenes. The antitumor drug iron-bleomycin – a metallo-glycopeptide – causes oxidative DNA cleavage [6,7] and also oxidizes a wide variety of organic substrates [6,8]. Thus, the synthesis of low molecular weight metal complexes aiming to mimic key – structural and – functional properties of natural enzymes is a topic of considerable interest. Of particular, demand is to achieve catalytic efficiency using green oxidants e.g. like $H_2O_2$ or $O_2$ [7,9–13]. In this context, stereoselective hydroxylation, epoxidation and *cis*-dihydroxylation by synthetic biomimetic catalysts have been reported [14–22].

In several bioinspired iron-based oxidation catalysts Fe-peroxo species have been invoked to be formed during the catalytic reaction [23,24]. More particularly, a $Fe^{III}$–OOH intermediate has been suggested as key-specie in oxidation reactions of several biomimetic non-heme iron complexes [9]. The formation of the $Fe^{III}$–OOH intermediate is a result of $H_2O_2$ deprotonation and subsequent ligation to the $Fe^{III}$ center. This $Fe^{III}$–OOH species is the precursor for a high-valent Fe-oxo species, which is responsible for substrate oxidation [2]. Three main pathways can be considered for the cleavage of the O–O bond [25]. (a) Homolytic cleavage leads to a $Fe^{IV}$=O species plus a short-lived highly reactive •OH radical, which is immediately transferred to the substrate [25]. (b) Heterolytic cleavage of the O–O bond generates a $Fe^{v}$=O (analogous to heme-peroxidase) [26] and a $OH^-$ species. (c) Finally, the $Fe^{III}$–OOH intermediate itself could be involved in substrate oxidation providing an oxidant with moderate reactivity and higher selectivity [27,28].

The heterogenization of catalysts, in contemporary environmentally conscious days, provides important 'green benefits' e.g. when solvent and catalyst losses during separation lead to unacceptable waste levels [29]. Thus, replacement of a homogeneous catalyst by an active heterogeneous one changes the synthetic process towards a more desirable and clean one. This provides advantages e.g. easy-handling, easy product separation, catalyst recovery and waste minimization [30]. However, very few literature reports are available on active heterogeneous non-heme iron catalysts functioning with $H_2O_2$ [31,32].

In the present work (a) we report the synthesis and catalytic evaluation of (i) a homogeneous **L**$Fe^{III}$Cl and (ii) the heterogeneous **L**$Fe^{III}$·$SiO_2$ catalyst. **L** stands for 3-{2-[2-(3-hydroxy-1,3-diphenyl-allylideneamino)-ethylamino]-ethylimino}-1,3-diphenyl-propen-1-ol (Scheme 1). Catalytic oxidations were evaluated using $H_2O_2$. (b) The stability of the catalysts has been also studied. Significant recyclability was found

* Corresponding author.
*E-mail addresses:* ideligia@cc.uoi.gr (Y. Deligiannakis), mlouloud@uoi.gr (M. Louloudi).

0920-5861/$ – see front matter © 2010 Elsevier B.V. All rights reserved.
doi:10.1016/j.cattod.2010.03.063

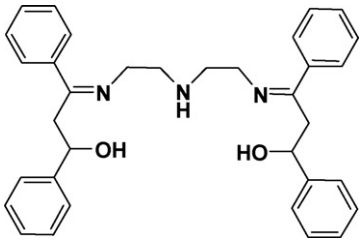


**Scheme 1.** The ligand [3-{2-[2-(3-hydroxy-1,3-diphenyl-allylideneamino)-ethylamino]-ethylimino}-1,3-diphenyl-propen-1-ol] (**L**) used herein to form the **L**$Fe^{III}$ catalysts for hydrocarbon oxidation with $H_2O_2$.

for the heterogeneous **L**$Fe^{III}$·$SiO_2$ catalyst. (c) UV–vis kinetic data suggest formation of **L**$Fe^{III}$–OOH species and EPR data show that in the presence of $CH_3CN$, low-spin $Fe^{III}$ ($S = 1/2$) centers are formed, which are responsible for the catalytic activity. The synthesis and characterization of the ligand **L** has been reported in our recent reports [33,34] (Scheme 1).

## 2. Experimental

All substrates were purchased from Aldrich, in their highest commercial purity, stored at 5 °C and purified by passage through a column of basic alumina prior to use. Thirty percent aqueous solution of hydrogen peroxide was used. Infrared spectra were recorded on a spectrum GX PerkinElmer FT-IR System. UV–vis spectra were recorded using a UV/VIS/NIR JASCO spectrophotometer and a PerkinElmer Lamda 35 with a diffuse reflectance setup. Fe quantitation was done by Flame Atomic Absorption Spectroscopy (FAAS) on a PerkinElmer AAS-700 spectrometer. Mössbauer spectra were recorded with a constant acceleration spectrometer using a $^{57}$Co(Rh) source at room temperature and a variable temperature. X-Band Electron Paramagnetic Resonance (EPR) spectra were recorded using a Brucker ER200D spectrometer at liquid $N_2$ temperatures, equipped with an Agilent 5310A frequency counter running under a home-made software based on LabView described earlier [35]. Mass spectra were measured on an Agilent 1100 Series LC-MSD-Trap-SL spectrometer and solution. GC analysis was performed using an 8000 Fisons chromatograph with a flame ionization detector and a Shimadzu GC-17A gas chromatograph coupled with a GCMS-QP5000 mass spectrometer.

Details about catalyst's preparation and characterization, catalytic experiments, UV–vis and EPR sample preparation are given in Supporting Information.

## 3. Results and discussion

### 3.1. Hydrocarbon oxidation by the homogeneous and heterogeneous *L*$Fe^{III}$ catalysts

The catalytic properties of the homogeneous **L**FeCl and heterogeneous **L**Fe·$SiO_2$ catalysts have been evaluated for hydrocarbon oxidation with $H_2O_2$. The oxidation reactions were carried out at room temperature under Ar atmosphere. When the catalytic experiments took place under air, $O_2$ affected both yield and selectivity of the oxidation products. Thus, in the data shown herein all the catalytic reactions were studied under strict inert Ar atmosphere. The catalytic data are summarized in Table 1, and Fig. 1 provides a histogram of them.

Based on Table 1, both the homogeneous and heterogeneous catalysts were efficient in alkene oxidations providing significant yields. More specifically, cyclohexene and limonene oxidation catalyzed by the **L**FeCl provided oxidation products with a combined

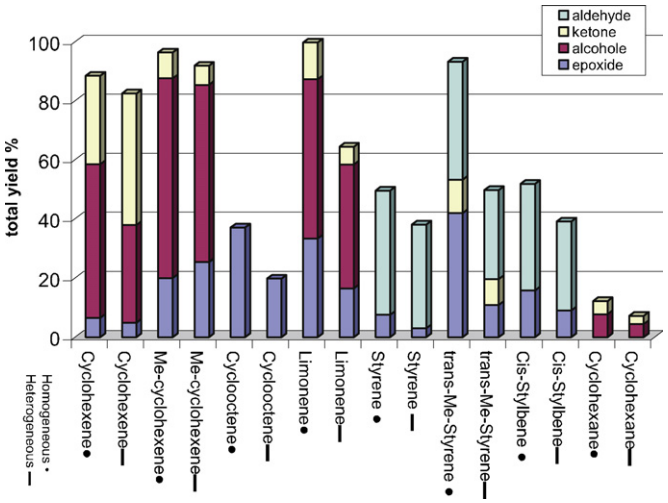


**Fig. 1.** Distribution of oxidation products catalyzed by **L**FeCl and **L**Fe·$SiO_2$ in $CH_3CN$ in the presence of $H_2O_2$. See Table 1 for further details.

yield of 88.5% and 99.8% respectively, while the same reactions catalyzed by the **L**Fe·$SiO_2$ gave combined yields of 82.5% and 64.5%. Cyclohexene undergoes mainly allylic oxidation forming 2-cyclohexene-1-ol and 2-cyclohexene-1-one. However cyclohexene epoxidation was also observed, with low epoxide yields. The major products detected from limonene oxidation were (i) two epoxides (*cis* and *trans*) originating from epoxidation of the electron-rich double bond in 1,2-position, (ii) alcohols derived from hydroxylation of the double bond in 1- and 2-position and from hydroxylation in 6-position close to 1,2-double bond. Oxidation products from the more accessible, but less electron-rich, double bond at 8,9-position were not observed. Additionally, considerable amounts of the corresponding ketone at 6-position were also formed (see details in Table 1). Methyl-substituted alkenes were more reactive, in both epoxidation and allylic oxidation. Thus, in the case of methyl-cyclohexene, the detected oxidation products were *cis*-epoxide, 1-methyl-2-cyclohexen-1-ol, 3-methyl-2-cyclohexen-1-ol and 3-methyl-2-cyclohexen-1-one. The total yield of methyl-cyclohexene oxidation products was 96.4% and 91.9% by **L**FeCl and **L**Fe·$SiO_2$ respectively. *Cis*-cyclooctene as substrate afforded a single-product reaction e.g. giving only the *cis*-cyclooctene epoxide with 37.0% and 19.8% yield catalyzed by **L**FeCl and **L**Fe·$SiO_2$ respectively (Fig. 1). In the oxidation of *cis*-stilbene, the major product was benzaldehyde as oxidative cleavage product (36.0% and 30.0% by **L**FeCl and **L**Fe·$SiO_2$ respectively). Considerable amounts of *cis*-stilbene epoxide (15.8% in homogeneous and 9.0% in heterogeneous medium) have been also detected. Styrene oxidation provided also benzaldehyde as major product deriving from oxidative cleavage of the exo-cyclic double bond. However, epoxide and phenyl acetaldehyde have been also formed e.g. by direct oxidation of the same double bond. Overall, styrene was oxidized by **L**FeCl and **L**Fe·$SiO_2$ with total oxidation yields of 49.5% and 38.0% respectively. The methyl-substituted styrene, *trans*-β-methyl styrene is more reactive providing total oxidation yields of 93.2% and 49.7% by **L**FeCl and **L**Fe·$SiO_2$ respectively. The identified products were *trans*-epoxide, methyl-benzyl-ketone and benzaldehyde as oxidation cleavage adduct.

Finally, cyclohexane oxidation gave cyclohexanol and cyclohexanone with combined yields of 12.2% and 7.2% and an alcohol/ketone (A/K) ratio of 1.75 and 1.60 for the **L**$Fe^{III}$Cl and the **L**$Fe^{III}$·$SiO_2$ catalyst respectively. The A/K ratio in cyclohexane can be used as a criterion for the presence and lifetime of free alkyl radical intermediates [24] as follows. (i) When A/K = 1, it assumes that the alkyl radicals are long-lived with a strong tendency to interact

**Table 1**
Hydrocarbon oxidation catalyzed by **L**FeCl and **L**Fe·$SiO_2$ with $H_2O_2$.

| Substrate | Products | **L**FeCl[c] yield (%) | **L**Fe·$SiO_2$[d] yield (%) | **L**FeCl[c] total yield (%) | **L**Fe·$SiO_2$[d] total yield (%) |
|---|---|---|---|---|---|
| Cyclohexene[a] | *cis*-Epoxide | 6.5 | 4.9 | | |
| | 2-Cyclohexenol | 52.0 | 32.9 | | |
| | 2-Cyclohexenone | 30.0 | 44.7 | 88.5 | 82.5 |
| 1-Methyl-cyclohexene[a] | *cis*-Epoxide | 20.0 | 25.4 | | |
| | 1-Methyl-2-cyclohexen-1-ol | 25.6 | 27.7 | | |
| | 3-Methyl-2-cyclohexen-1-ol | 42.0 | 32.3 | | |
| | 3-Methyl-2-cyclohexen-1-one | 8.8 | 6.5 | 96.4 | 91.9 |
| Cyclooctene[a] | *cis*- Epoxide | 37.0 | 19.8 | 37.0 | 19.8 |
| Limonene[a] | *cis*-1,2 Epoxide | 21.0 | 8.5 | | |
| | *trans*-1,2 Epoxide | 12.3 | 8.0 | | |
| | Limonene alcohol[e] | 54.0[f] | 41.9[g] | | |
| | Limoneme ketone[h] | 12.5 | 6.0 | 99.8 | 64.4 |
| Styrene[b] | Epoxide | 7.5 | 3.0 | | |
| | Phenyl acetaldehyde | 7.0 | 3.0 | | |
| | Benzaldehyde | 35.0 | 32.0 | 49.5 | 38.0 |
| Methyl-styrene[b] | *trans*-Epoxide | 41.9 | 10.9 | | |
| | Methyl-benzyl-ketone | 11.3 | 8.8 | | |
| | Benzaldehyde | 40.0 | 30.0 | 93.2 | 49.7 |
| *cis*-Stylbene[b] | *cis*-Epoxide | 15.8 | 9.0 | | |
| | Benzaldehyde | 36.0 | 30.0 | 51.8 | 39.0 |
| Cyclohexane[a] | Cyclohexanol | 7.7 | 4.5 | | |
| | Cyclohexanone | 4.4 | 2.8 | 12.2 | 7.2 |

[a] Conditions: ratio of catalyst:$H_2O_2$:substrate = 1:20:1000.
[b] Conditions: ratio of catalyst:$H_2O_2$:substrate = 1:50:1000.
[c] Reaction was completed within 4 h.
[d] Reaction was completed within 24 h.
[e] Limonene alcohols were found to be a mixture of 1-ol, 2-ol and 6-ol.
[f] 54% yield corresponds to 23% for 1-ol, 13.5% for 2-ol and 17.5% for 6-ol.
[g] 41.9% yield corresponds to 25.3% for 1-ol, 6.9% for 2-ol and 10.0% for 6-ol.
[h] The only observed ketone is the 6-one.

with $O_2$ to form alkyl-peroxy-radicals [25]. At the end, following a Russell-type terminal stage [36], recombination of these radicals results in the formation of equimolar amounts of alcohol and ketone [14,24]. (ii) When the A/K > 1, the radical •OH is formed by a metal-based system and the metal center reacts directly to form the corresponding alcohol.

### 3.2. Catalysts stability

The efficiency and stability of $Fe^{III}$ catalysts under operating conditions were studied by progressive addition of $H_2O_2$ to cyclohexene in $CH_3CN$. The starting molar ratio [catalyst:$H_2O_2$:substrate] was [1:20:1000]. After the end of each oxidation reaction an additional amount of 20 equiv. of $H_2O_2$ was added. The results are presented in Fig. 2.

#### 3.2.1. Homogeneous catalyst

According to Fig. 2, in the oxidation reaction catalyzed by the **L**FeCl, the first 20 equiv. of $H_2O_2$ resulted in 17.7 tons. The addition of a second dose of 20 equiv. of $H_2O_2$ caused a yield increase to 23.7 tons. Third addition of oxidant improved slightly the total tons to 28.3. Overall, the data in Fig. 2 (solid symbols) indicate that the evolution of the catalytic reaction catalyzed by the **L**FeCl has practically stopped during the second run. Probably this was due to catalyst destruction. This is strongly evidenced by discoloration of the orange reaction mixture and MS-detection of molecular-fragments derived from **L**FeCl.

#### 3.2.2. Heterogeneous catalyst

In the oxidation reaction catalyzed by the **L**Fe·$SiO_2$, the first 20 equiv. of $H_2O_2$ resulted in 16.5 tons (Fig. 2 open symbols). In contrast to **L**FeCl, in the case of the **L**Fe·$SiO_2$ addition of $H_2O_2$ caused an almost linear increase of the tons, up to the fourth dose of $H_2O_2$ (Fig. 2). Noticeably, turnover numbers approached a value of 40.2 for 80 equiv. of $H_2O_2$. Remarkably, the **L**Fe·$SiO_2$ was active after the addition of a fifth amount of 20 equiv. of $H_2O_2$. Even a sixth one provides new amounts of oxidation products (Fig. 2). No catalyst degradation has been detected by MS. Overall the data in Fig. 2 and the MS-data demonstrate that under the catalytic conditions used, the **L**Fe·$SiO_2$ was much more stable than the homogeneous **L**Fe catalyst. These findings encouraged us to investigate in more detail the recyclability of the **L**Fe·$SiO_2$ catalyst.

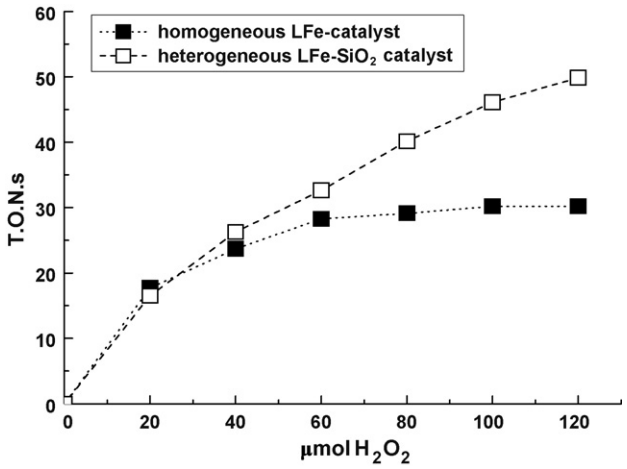


**Fig. 2.** Cyclohexene oxidation upon progressive addition of $H_2O_2$ catalyzed by homogeneous **L**FeCl (solid symbols) and heterogeneous **L**Fe·$SiO_2$ (open symbols) catalysts.

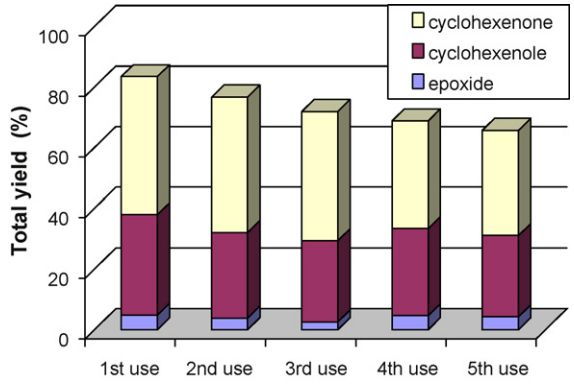


**Fig. 3.** Bar chart representation of cyclohexene oxidation catalyzed by recycled **L**Fe·$SiO_2$.

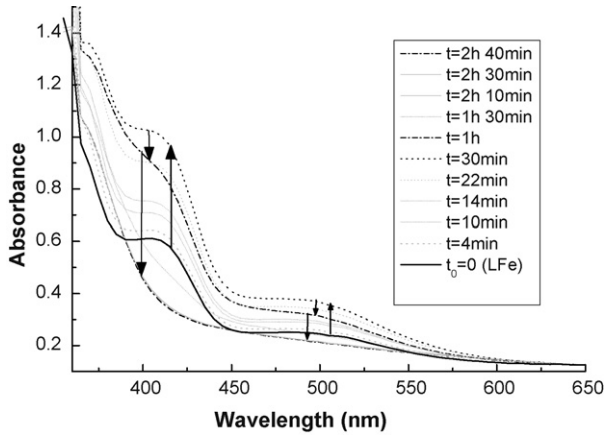


**Fig. 4.** Evolution of catalytic cyclohexene oxidation in $CH_3CN$ with $H_2O_2$.

### 3.3. Recyclability of the heterogeneous **L**Fe·$SiO_2$ catalyst

The recycling and regenerating ability of the **L**Fe·$SiO_2$ were tested using cyclohexene as substrate, in $CH_3CN$, for a [catalyst:$H_2O_2$:substrate] = [1:20:1000]. After the end of each oxidation reaction, the solid catalyst was isolated from the reaction mixture by filtration, washed with $CH_3CN$ and dried under pressure (80 °C, 2 h). Subsequently the recovered solid catalyst was reused for a new oxidation reaction under the same catalytic conditions. The catalytic data obtained by this set of experiments are displayed in Fig. 3. The data in Fig. 3 shows that (a) after repetitive uses the recycled catalyst was able to activate $H_2O_2$ in the new catalytic reaction. (b) A progressive loss by ~4% of activity was observed *per use*: from 80% (in 1st use) the total yield was 76% (in 2nd use) and progressively was decreasing in a quasilinear way e.g. after the 5th re-use the total yield was ~60%. (c) Importantly in all the uses the same distribution of oxidation products was observed. The DR-UV–vis spectrum of the 5-times used **L**Fe·$SiO_2$ was comparable with the spectrum of the non-used **L**Fe·$SiO_2$ catalyst. In addition, no catalyst degradation has been detected by MS. Overall, we consider that the 4% activity loss *per use* shows that the heterogeneous **L**Fe·$SiO_2$ catalyst presents good recyclability behavior. An analogous stability enhancement has been reported by us [33,34] and other researchers [37,38] for other catalysts supported on $SiO_2$. Thus we consider that the silica support probably protects the active catalyst centers against oxidation destruction.

### 3.4. Changes in UV–vis spectrum of **L**$Fe^{III}$ in the presence of $H_2O_2$

The progress of cyclohexene oxidation with $H_2O_2$ catalyzed by **L**FeCl was monitored by UV–vis spectroscopy at 0 °C, for [catalyst:$H_2O_2$:cyclohexene] = [1:20:1000]. Final catalyst concentration was 0.33 mM in $CH_3CN$. At 0 °C after completion of $H_2O_2$ addition, the bands at 413 and 512 nm – attributed to LMCT – were progressively increased in intensity and slightly blue shifted (solid line). This was continued for 30 min (upward-arrows in Fig. 4). After this period, a decrease in the bands at 413 and 512 nm was observed (downward-arrows in Fig. 4). Finally, after 200 min, these bands were no longer detectable (dashed-dotted line). The observed spectral changes in Fig. 4 parallel the observation reported previously [16,22,39,40]. According to reference [39], spectral changes such as in Fig. 4, confirm the interaction between the Fe complex and the $H_2O_2$ involved in the catalytic process [39]. Thus, on the basis of the UV–vis kinetic data after oxidant addition, formation and concomitant consumption of an **L**$Fe^{III}$–OOH species might be concluded [16,22,39,40] (Fig. 4).

### 3.5. Catalysis monitored by EPR spectroscopy

A Mössbauer spectrum for **L**$Fe^{III}$Cl powder is shown in Fig. 5A. The presence of only one doublet in conjunction with Fe-analysis is clear evidence for the formation of a mononuclear $Fe^{III}$-complex. At 77 K, the Mössbauer parameters were $\delta = 0.50$ mm/s and $\Delta_{EQ} = 0.54$ mm/s indicating an octahedral high-spin $Fe^{III}$ ($S = 5/2$) center, with the iron bound to N- and O-atom donors [41]. The EPR spectrum of solid **L**$Fe^{III}$Cl was characterized by two peaks at $g = 4.3$ and 9.2 characteristic of a high-spin (HS) $Fe^{III}$ ($S = 5/2$) center in a rhombic ligand-field characterized by E/D~0.33 [42]. Fig. 6 shows low temperature X-Band EPR spectra of **L**FeCl in different solvents. The EPR spectra of all samples contained a signal cen-

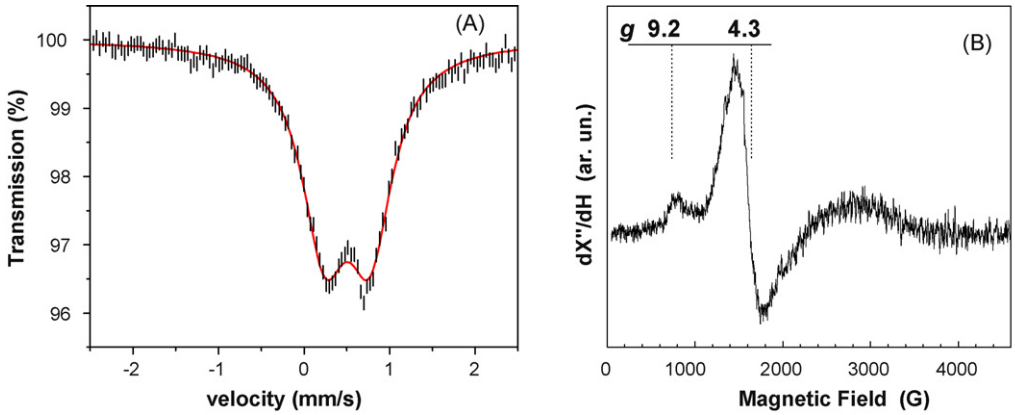


**Fig. 5.** Mössbauer (A) and EPR (B) spectrum for **L**FeCl. Temperature 77 K.

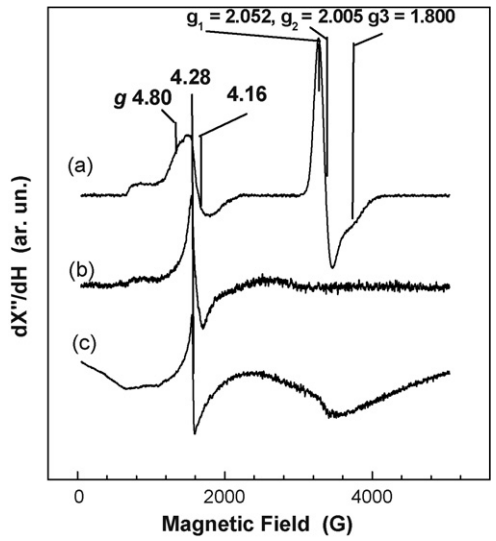


**Fig. 6.** EPR spectra of **L**Fe complex (a) in $CH_3CN$, (b) in MeOH, (c) in $CH_2Cl_2$. Experimental conditions: modulation amplitude 10 G, microwave power 32 mW, modulation frequency 100 Kh, temperature 77 K.

tered at $g = 4.3$. This signal is characteristic of a typical non-heme high-spin $Fe^{III}$ ($S = 5/2$). A close inspection of Fig. 6 reveals small differences between the HS $Fe^{III}$ signals indicating the formation of HS $Fe^{III}$ species with different ligand-field E/D rhombicity ratios [42]. According to the $g$-values, in the presence of $CH_3CN$ the E/D rhombicity ratio is 0.25 [42] while in MeOH or $CH_2Cl_2$ E/D~0.33 [42] (Fig. 6). In $CH_3CN$, a strong EPR signal centered at 3345 G was also detected (Fig. 6, spectrum (a)) at the expense of the $g$~4.3 signal. The new $Fe^{III}$ state is characterized by $g$-values: $g_1 = 2.052$, $g_2 = 2.005$ and $g_3 = 1.80$ and is assigned to low-spin (LS) $Fe^{III}$ ($S = 1/2$) complexes. Based on the HS and LS EPR signals in Fig. 6 we estimate that 40% of the Fe centers are in the LS state while 60% remained in the HS state. The LS signal was absent at the EPR spectra of the **L**FeCl in MeOH or $CH_2Cl_2$. Formation of LS $Fe^{III}$ ($S = 1/2$) has been previously reported for non-heme iron complexes in $CH_3CN$ [16,43]. Coordination of $CH_3CN$ to non-heme iron complexes leading to the formation of LS states has been documented by crystallographic data also [16,43]. Overall, it is concluded that for the formation of the LS state, $CH_3CN$ must be used as solvent, which occupies the sixth coordination site. Based on the $g$-values of the low-spin $Fe^{III}$ specie the rhombicity ($V/\Delta$) parameters are 1.3. The tetragonality ($\Delta/\lambda$) parameter – which depends primarily on the detailed balance of the charge of the iron atom – is 6.2. Similar EPR spectra of low-spin ferric complex with rhombic character have been observed [44]. Fig. 7A shows the time dependence of the EPR intensity of the LS $Fe^{III}$ signal in the presence of 5 and 20 equiv. of $H_2O_2$ with respect to the catalyst and in the absence or presence of substrate. In the presence of substrate and 20 equiv. $H_2O_2$, the LS $Fe^{III}$ signal decreased rapidly, disappearing within 2 min. On the other hand, with 5 equiv. of $H_2O_2$ a 70% decrease of the initial LS signal was observed within 10 min incubation time. In both cases, beside the decrease of the EPR intensity no other changes were detected in the EPR spectra. Oxidation of the iron and formation of an EPR silent species could take place. A third sample was also prepared containing 1000 equiv. of the substrate with respect to the catalyst incubated for 10 min, and 20 equiv. of $H_2O_2$ (Fig. 7A (△)). In this case, a variation of the EPR intensity of the LS $Fe^{III}$ signal was observed. However, the signal was constantly present contrary to the case where the substrate was added. Fig. 7B shows the effect of $H_2O_2$ and substrate on the time dependence of the HS $Fe^{III}$ signal's intensity. With 5 equiv. of $H_2O_2$ an increase of the HS $Fe^{III}$ was observed. In contrast, a gradual decrease of the LS EPR signal was observed (Fig. 7A). In the presence of 20 equiv. of $H_2O_2$ with respect to the catalyst an increase was also observed at short incubation times (i.e. $t < 0.5$ min), followed by constant decrease. However, the decay of the HS state was much slower than the LS state. Differences on the time dependence of the LS and HS $Fe^{III}$ signal's intensity were also observed in the presence of the substrate. Contrary to the case of the LS state, the HS $Fe^{III}$ intensity remained approximately unchanged with 20 equiv. of $H_2O_2$ (Fig. 7B (△)).

The differences of the time depended intensity between the LS and HS states of $Fe^{III}$ with respect to 5 and 20 equiv. indicate that the HS state has higher redox potential than the LS state. Furthermore, the variation of the LS and the unchanged intensity of the HS state under the conditions of the catalytic experiments, indicate that the catalytic performance most likely depends on the LS state of the **L**FeCl rather than the HS. This hypothesis is supported by the higher

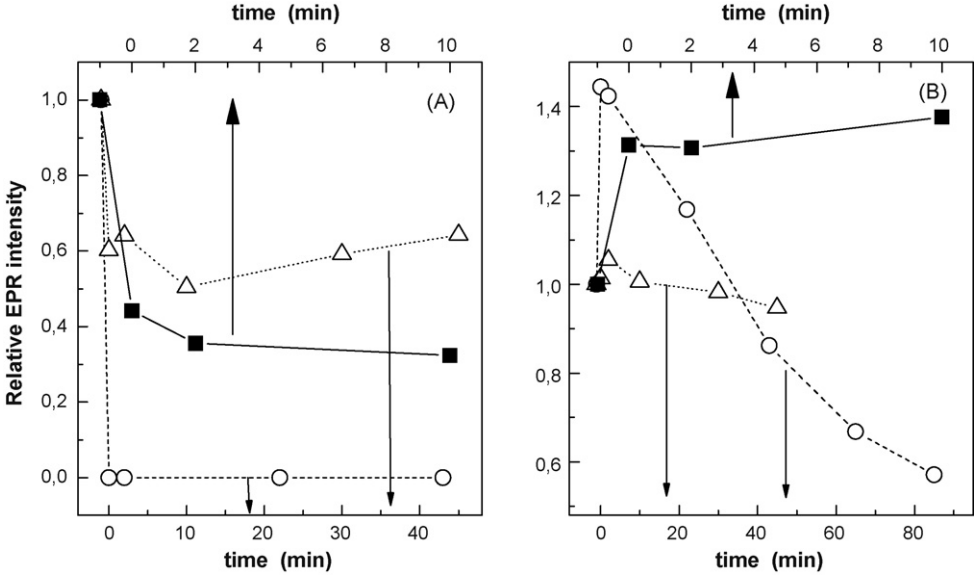


**Fig. 7.** Relative EPR intensity of (A) the low-spin $Fe^{III}$ and (B) the high-spin $Fe^{III}$. Experimental condition: 0.2 mM **F**e$L_1$ in $CH_3CN$ in the presence of 1 mM $H_2O_2$ (solid line (■)) 4 mM $H_2O_2$ (dashed line (○)) and 200 mM substrate followed by the addition of 4 mM $H_2O_2$ (dotted line (△)).

catalytic performance of the catalyst when $CH_3CN$ is used as solvent compared with the cases of MeOH and $CH_2Cl_2$.

## 4. Conclusion

In $CH_3CN$ both the homogeneous and heterogeneous catalysts were efficient in alkene oxidations providing significant yields. In cyclohexane oxidation an alcohol/ketone (A/K) ratio of 1.75 and 1.60 was found by **L**$Fe^{III}Cl$ and **L**$Fe^{III}{\cdot}SiO_2$ catalysts respectively. UV–vis kinetic data suggest formation and concomitant consumption of a **L**$Fe^{III}$–OOH species. EPR data show that in $CH_3CN$, low-spin $Fe^{III}$ ($S = 1/2$) centers are formed, which are responsible for the catalytic activity. Under the catalytic conditions used, the **L**$Fe{\cdot}SiO_2$ was much more stable than the homogeneous **L**Fe catalyst. The recycled **L**$Fe{\cdot}SiO_2$ catalyst (a) was able to activate $H_2O_2$ in to the new catalytic reaction, (b) when tested for up to 5 re-uses, showed a total yield loss ~4% *per use*, providing the same distribution of oxidation products.

## Appendix A. Supplementary data

Supplementary data associated with this article can be found, in the online version, at doi:10.1016/j.cattod.2010.03.063.

## References

[1] M. Merkx, D.A. Kopp, M.H. Sazinsky, J.L. Blazyk, J. Muller, S.J. Lippard, Angew. Chem. Int. Ed. 40 (2001) 2782–2807.
[2] B.J. Wallar, J.D. Lipscomb, Chem. Rev. 96 (1996) 2625–2657.
[3] S.C. Pulver, W.A. Froland, J.D. Lipscomb, E.I. Solomon, J. Am. Chem. Soc. 119 (1997) 387–395.
[4] M.D. Wolfe, J.V. Parales, D.T. Gibson, J.D. Lipscomb, J. Biol. Chem. 276 (2001) 1945–1953.
[5] A. Karlsson, J.V. Parales, R.E. Parales, D.T. Gibson, H. Eklund, S. Ramaswamy, Science 299 (2003) 1039–1042.
[6] R.M. Burger, Chem. Rev. 98 (1998) 1153–1169.
[7] E.I. Solomon, T.C. Brunold, M.I. Davis, J.N. Kemsley, S.-K. Lee, N. Lehnert, F. Neese, A.J. Skulan, Y.-S. Yang, J. Zhou, Chem. Rev. 100 (2000) 235–349.
[8] C.A. Claussen, E.C. Long, Chem. Rev. 99 (1999) 2797–2816.
[9] L. Que, W.B. Tolman, Bio-coordination chemistry, in: J.A. McCleverty, T.J. Meyer (Eds.), Comprehensive Coordination Chemistry II, vol. 8, Elsevier, Oxford, UK, 2004.
[10] E.Y. Tshuva, S.J. Lippard, Chem. Rev. 104 (2004) 987–1012.
[11] A.L. Feig, S.J. Lippard, Chem. Rev. 94 (1994) 759–805.
[12] C. He, Y. Mishina, Curr. Opin. Chem. Biol. 8 (2004) 201–208.
[13] J.-U. Rohde, M.R. Bukowski, L. Que, J. Curr. Opin. Chem. Biol. 7 (2003) 674–682.
[14] K. Chen, L. Que, Chem. Commun. 15 (1999) 1375–1376.
[15] M. Costas, A.K. Tipton, K. Chen, D.-H. Jo, L. Que, J. Am. Chem. Soc. 123 (2001) 6722–6723.
[16] K. Chen, M. Costas, J. Kim, A.K. Tipton, L. Que, J. Am. Chem. Soc. 124 (2002) 3026–3035.
[17] P.D. Oldenburg, A.A. Shteinman, L. Que, J. Am. Chem. Soc. 127 (2005) 15672–15673.
[18] C.P. Horwitz, D.R. Fooksman, L.D. Vuocolo, S.W. Gordon-Wylie, N.J. Cox, J.T. Collins, J. Am. Chem. Soc. 120 (1998) 4867–4868.
[19] J.T. Collins, Acc. Chem. Res. 35 (2001) 782–790.
[20] J.M. Rowland, M. Olmstead, P.K. Mascharak, Inorg. Chem. 40 (2001) 2810–2817.
[21] M. Klopstra, G. Roelfes, R. Hage, R.M. Kellog, B.L. Feringa, Eur. J. Inorg. Chem. 4 (2004) 846–856.
[22] F.G. Gelalcha, G. Anilkumar, M.K. Tse, A. Brücknerc, M. Beller, Chem. Eur. J. 14 (2008) 7687–7698.
[23] L. Que Jr., R.Y.N. Ho, Chem. Rev. 96 (1996) 2607–2624.
[24] M. Costas, K. Chen, L. Que Jr., Coord. Chem. Rev. 200–202 (2000) 517–544.
[25] S. Tanase, E. Bouwman, Adv. Inorg. Chem. 58 (2006) 29–75.
[26] M. Sono, M.P. Roach, M.P. Coulter, J.H. Dawson, Chem. Rev. 96 (1996) 2841–2887.
[27] P.R. Ortiz de Montellano, Acc. Chem. Res. 31 (1998) 543–549.
[28] G. Roelf, M. Luben, R. Hage, L. Que, B.L. Feringa, Chem. Eur. J. 6 (2000) 2152–2159.
[29] J.H. Clark, Green Chem. 1 (1999) 1–8.
[30] M.H. Valkenberg, W.F. Holderich, Catal. Rev. 44 (2002) 321–374.
[31] A. Dhakshinamoorthy, K. Pitchumani, Tetrahedron 62 (2006) 9911–9918.
[32] K.C. Gupta, A.K. Sutar, C.-C. Lin, Coord. Chem. Rev. 253 (2009) 1926–1946.
[33] M. Louloudi, K. Mitopoulou, E. Evaggelou, Y. Deligiannakis, N. Hadjiliadis, J. Mol. Catal. A: Chem. 198 (2003) 231–240.
[34] Ch. Vartzouma, E. Evaggellou, Y. Sanakis, N. Hadjiliadis, M. Louloudi, J. Mol. Catal. A: Chem. 263 (2007) 77–85.
[35] G. Grigoropoulou, K.C. Christoforidis, M. Louloudi, Y. Deligiannakis, Langmuir 23 (2007) 10407–10418.
[36] F. Gozzo, J. Mol. Catal. A: Chem. 171 (2001) 1–22.
[37] W. Xue, J.C. Zhang, Y.J. Wang, Catal. Commun. 6 (2005) 431–436.
[38] R.X. Wang, W.Z. Jiao, B.J. Gao, Appl. Surf. Sci. 255 (2009) 7766–7772.
[39] G.C. Silva, G.L. Parrilha, N.M.F. Carvalho, V. Drago, C. Fernandes, A. Horn Jr., O.A.C. Antunes, Catal. Today 133–135 (2008) 684–688.
[40] G. Roelfes, M. Lubben, K. Chen, R.Y.N. Ho, A. Meetsma, S. Genseberger, R.M. Hermant, R. Hage, S.K. Mandal, V.G. Young, Y. Zang, H. Kooijman, A.L. Spek, L. Que, B.L. Feringa, Inorg. Chem. 38 (1999) 1929–1936.
[41] D.P.E. Dickson, F.J. Berry, Mossbauer Spectroscopy, Cambridge University Press, 1996.
[42] J. Peisach, W.E. Blumberg, S. Ogawa, E.A. Rachmilewitz, R. Oltzik, J. Biol. Chem. 246 (1971) 3342.
[43] M.P. Jensen, S.J. Lange, M.P. Mehn, L. Que, J. Am. Chem. Soc. 125 (2003) 2113–2128.
[44] L. Duelund, H. Toftlund, Spectrochim. Acta A 56 (2000) 331–340.